

## Optical properties of V, Ta, and Mo from 0.1 to 35 eV

J. H. Weaver,\* D. W. Lynch, and C. G. Olson

Ames Laboratory, United States Atomic Energy Commission and Department of Physics, Iowa State University, Ames, Iowa 50010

(Received 26 December 1973)

The absorptivity or reflectivity of crystals of V, Ta, and Mo was measured from 0.1 to 35 eV. The data were Kramers-Kronig analyzed to determine the dielectric functions. The inadequacy of a simple Drude model to describe absorption at low energy is discussed. Structure in the dielectric functions is discussed in terms of direct interband transitions which extend to about 18 eV. Features below 6 eV are attributed to transitions near  $\Sigma$ ,  $G$ , and perhaps along  $P(D)N$  for V, Ta, and Mo, with additional transitions in Mo from the  $\Delta$  portion of the Brillouin zone. High-lying energy bands are identified as giving rise to high-energy structure in the dielectric functions. Results obtained previously for Nb are reviewed and compared. The electron-energy-loss functions were calculated and are discussed in terms of volume and surface plasmons. These metals all exhibit two volume and two surface plasmons.

### I. INTRODUCTION

The understanding of the electronic properties of the transition metals lags far behind that of the simple and noble metals. In part, this is due to the technical difficulties in obtaining high-purity samples for experimental study, but an equally formidable barrier for the theorist has been the very nature of the nonlocalized  $d$  electrons. Recently, improved schemes for devising and constructing appropriate potentials to be used in the calculations of the energy bands have made those calculations more reliable.<sup>1-3</sup> Such theoretical studies have become feasible as the store of experimental data has grown. Such highly sensitive experimental probes as the de Haas-van Alphen (dHvA) effect have proved valuable for mapping the Fermi surfaces of many of the transition metals. A further understanding of the electronic properties can be gained from a thorough study of the optical properties of the metals. It was with this in mind that the present studies were undertaken. This paper represents our ongoing interest in the transition metals in general and the bcc metals in particular.<sup>4-6</sup> After a brief review of some of the theoretical and experimental studies of V, Ta, and Mo, we will present our optical reflectivity data, discuss the Kramers-Kronig analysis of those data, and try to interpret the dielectric functions in terms of existing band calculations.

Most of the experimental studies of V and its Fermi surface have come within the last few years. The paucity of experimental information prior to then did not warrant complete band calculations, but recently a variety of theoretical studies have appeared.

The optical properties of V were considered by Bolotin *et al.*<sup>7</sup> They measured  $n$  and  $k$ , the real and imaginary parts of the complex refractive index, ellipsometrically between 2 and 9  $\mu\text{m}$  at room temperature. Vilesov *et al.*<sup>8</sup> measured the reflectivity

between about 5 and 15 eV, but their results bear little resemblance to the more recent work of Seignac and Robin.<sup>9</sup> Seignac and Robin determined the optical properties based on their reflectivity measurements on V films between 3 and 50 eV (250 to 4000  $\text{\AA}$ ). Optical absorption measurements have also been reported between 30 and 300 eV by Sonntag *et al.*<sup>10</sup> which showed core levels about 50 eV below  $E_F$ . Information about the extent of the occupied  $d$  bands of V has come from photoemission studies of Eastman.<sup>11</sup>

The energy bands of V have been calculated with varying degrees of completeness. Mattheiss<sup>12</sup> displayed  $E(\mathbf{k})$  along  $\Gamma(\Delta)H$ , and Snow and Waber<sup>13</sup> considered V in conjunction with the  $3d$  series of transition metals. Neither work provided a detailed band scheme, although Mattheiss<sup>14</sup> did subsequently discuss the V group briefly in terms of the bands and Fermi surface of W. More recently, augmented-plane-wave (APW) calculations by Anderson *et al.*<sup>15</sup> showed the bands along  $N-\Gamma-H$  for two values of the exchange-potential coefficient and at normal and reduced lattice spacings. The same group<sup>16</sup> subsequently completed self-consistent APW calculations giving the bands at points of high symmetry. Yasui *et al.*<sup>17</sup> evaluated the self-consistent bands with two different exchange-term coefficients, treating the  $d$  electrons by a tight-binding method and the conduction bands by an orthogonalized-plane-wave (OPW) method. Hattox *et al.*<sup>18</sup> recently have calculated the bands of V at normal and reduced lattice spacings. Hodges<sup>19</sup> has calculated the bands of V, but the results have not yet been compared with experimental data. The various bands will be compared and discussed subsequently in conjunction with the optical data.

The Fermi surface of V has been studied by two groups using the technique of magnetoresistance. Alekseevskii and Egorov<sup>20</sup> reported practically no anisotropy, while Nelson *et al.*,<sup>21</sup> working with samples of higher purity, reported anisotropy.

Phillips<sup>22</sup> has performed dHvA measurements. Thermomodulation experiments<sup>23</sup> have been undertaken to provide detailed information about the bands near the Fermi level. Additional optical measurements have also been undertaken by Johnson and Christy.<sup>24</sup>

The existing optical experiments with Ta have been limited to the ultraviolet and visible regions of the spectrum. Juenker and co-workers<sup>25,26</sup> have determined the reflectivity of high-temperature-cleaned surfaces of rolled Ta metal. The absorption coefficient,  $\mu$ , of Ta has been determined by Haensel *et al.*<sup>27</sup> between about 30 and 600 eV.

The electronic structure of Ta was considered by Mattheiss<sup>3</sup> (APW method) in conjunction with studies of Nb. Niobium was considered in the non-relativistic limit, but relativistic effects were included for Ta. A considerable similarity was noted for the Fermi surfaces and the bands near the Fermi level. This has been supported experimentally by recent de Haas-van Alphen,<sup>28-30</sup> magnetothermal-oscillation,<sup>30</sup> and galvanometric<sup>31</sup> measurements. Our optical data further demonstrate the similarities, but not to the extent suggested by the similarities in their Fermi surfaces. (For a discussion of the optical properties of Nb, see Ref. 4.) Petroff and Viswanathan<sup>32</sup> have reported APW nonrelativistic calculations of the bands of Ta, W, and Mo.

Optical investigations of Mo have been carried out by a variety of groups. Kirillova *et al.*<sup>33</sup> investigated the range from 0.06 to 4.9 eV using an oriented single crystal and an ellipsometric technique at room temperature. In an earlier paper, Kirillova and others<sup>34</sup> reported a reflectivity spectrum  $R(E)$  for Mo extending to about 12 eV. The results were in reasonably good agreement with those reported by Juenker and co-workers.<sup>25,26</sup> Kapitsa, Udoyev, and Shirokikh<sup>35</sup> measured  $R$  from 1.4 to 11 eV, but their values appeared to be too low; Udoyev, Koz'yakova, and Kapitsa<sup>36</sup> subsequently published further studies which are in good agreement with ours. Kress and Lapeyre<sup>37</sup> reported results of photoemission studies and also measured  $R(E)$  between 0.5 and 14 eV, while Anderson *et al.*<sup>38</sup> measured  $R(E)$  from 1.9 to 4.8 eV on a very clean Mo single-crystal surface.

The reflectivity of Mo has recently been measured by Veal and Paulikas<sup>39</sup> in the 0.5-6-eV range. The conductivity resulting from Kramers-Kronig analysis was compared with that calculated by Koelling, Mueller, and Veal.<sup>40</sup> The data, both reflectivity and conductivity, are in good agreement with ours, including the Drude parameters. The assignment of transitions is similar. Koelling *et al.* also studied the location of transitions by considering only transitions originating or terminating in an energy window about the Fermi level,

making the assignment of transitions firmer.

The Fermi surface of Mo has been considered in detail both experimentally and theoretically. Numerous de Haas-van Alphen,<sup>41-43</sup> radio-frequency size-effect,<sup>44,45</sup> magnetoresistance,<sup>46-48</sup> anomalous-skin-effect,<sup>49</sup> magnetoacoustic-effect,<sup>50</sup> and cyclotron-resonance<sup>51</sup> measurements have probed its Fermi surface. The first major theoretical contribution came from Lomer<sup>52</sup> who proposed a model for the Cr group based on the APW bands by Wood for Fe<sup>53</sup>; Lomer<sup>54</sup> later modified the model and applied it to Mo alone. APW calculations for Cr, Mo, and W by Loucks<sup>55</sup> have provided a picture of the Fermi surface that is in qualitative agreement with the model of Lomer, but quantitatively the results are not reliable due to an error in the magnitude of the unit cell used in the calculations. It has been shown, moreover, that the band structures of Mo and W are quite similar if relativistic effects are ignored. Mattheiss<sup>56</sup> has calculated a reasonably detailed nonrelativistic band structure for W. Petroff and Viswanathan<sup>32</sup> reported nonrelativistic Mo bands. Most recently, Iverson and Hodges<sup>57</sup> have applied a tight-binding interpolation scheme to renormalized atom calculations to obtain the Mo bands. Spin-orbit effects have also been considered by Loucks<sup>55</sup> and Mattheiss<sup>56</sup> for W and by Iverson and Hodges for Mo.<sup>57</sup>

As indicated above, the recent interest in the transition metals has been stimulated both by improved calculational schemes and the availability of high-purity samples. While the optical properties of a material are of considerable interest, there have been no systematic optical measurements of the transition metals which have covered the wide frequency range from the free-electron or Drude region, through the interband region, and finally touching the core levels. Accordingly, this study of V, Ta, and Mo was undertaken.

## II. EXPERIMENTAL METHOD

The experimental technique has been discussed in previous papers (see in particular Refs. 58 and 59). The procedure followed in the present case is basically as discussed therein. A calorimetric method was used between 0.1 and 4.88 eV to determine the absorptivity ( $A = 1 - R$ ) at 4.2 K and 15° angle of incidence. In the vacuum ultraviolet (vuv), synchrotron radiation from the electron storage ring operated by the Physical Sciences Laboratory of the University of Wisconsin was used, and room-temperature reflectivity ( $R$ ) measurements were made at 10°, 45°, and 60° for *s*- and *p*-polarized radiation. (The radiation at the sample was 88% polarized.) The low-energy limit of the reflectivity measurements was determined by the grating used in the 1-m normal-incidence McPherson 225 monochromator. This limit was reduced from that in

Ref. 4 by using a 600-line/mm grating and a KBr filter. Measurements of  $R$  extended to energies as low as 3.1 eV, thereby providing a region of overlap with the calorimetric measurements.

Samples of V, Ta, and Mo were spark-cut from electron-beam-melted buttons of high-purity material obtained within the Ames Laboratory of the U. S. AEC. Typical sample dimensions were  $8 \times 12$  mm with a thickness of about 1 mm. While the samples were not single crystals,<sup>60</sup> most of the surface exposed to long wavelength radiation was a single crystallite (V and Mo); since the vuv beam was smaller, a single crystallite was illuminated. A qualitative analysis of the sample material showed that the primary contaminants were C, O, and N.<sup>61</sup> The residual resistivity ratio (RRR),  $[\rho(300 \text{ K})/\rho(4.2 \text{ K})]$ , was measured as a second gauge of the sample purity. The measured RRR was 200 for V, 21.7 for Ta, and 193 for Mo. The RRR for V was higher than any reported in the literature, the sample used by Nelson *et al.*<sup>21</sup> excepted.

After the crystals were cut to size, they were macroetched, then polished, ending with  $1\text{-}\mu\text{m}$  alumina abrasive with alcohol or water as a carrier. They were electropolished<sup>62</sup> and annealed<sup>63</sup> in Ar-filled (low-temperature annealing) or vacuum-sealed (high-temperature annealing) Ta capsules. After annealing, the samples were cleaned, reelectropolished, washed in acetone, absolute (ethyl) alcohol, and dried in a stream of high-purity  $\text{N}_2$ . The samples were exposed to the atmosphere for only about 3–5 min before being placed in the  $\text{N}_2$ -purged calorimeter and evacuated. For the vuv measurements, the samples were again electropolished, dried, and immediately transferred to the sample chamber. (However, V was ultimately treated differently. See Sec. III.)

Since the extent of the surface layer damaged by spark cutting and mechanical polishing was not known, we were careful to remove amounts in excess of approximately  $50 \mu\text{m}$ .<sup>64</sup> The samples were x rayed using a back-reflection Laue technique. The resulting Laue spots were sharply defined, indicating an unstrained surface.

The accuracy of the calorimetric measurements is about 1% of the value of  $A$  at 1 eV, falling to about 10% of  $A$  at 0.1 eV. The vuv reflectivity measurements are believed to be good to within 5–7% of the value of  $R$ . These estimates do not include the effects of oxide layers. Such layers can be shown to produce negligible errors in the infrared, where they are transparent. Measurements of samples stored in air for several months gave nearly identical infrared spectra. The effect of an oxide layer in the visible and ultraviolet is much greater, but these metals do not oxidize rapidly, nor does a thick oxide layer build up. Our

samples probably are covered by a thin oxide. Repeated measurements, with the sample not removed from the sample chamber, gave reflectivities identical with earlier results, so equilibrium seems to have been obtained. Some measurements were made on opaque evaporated films. These gave lower reflectivities in all spectral regions.

### III. RESULTS

The results of the calorimetric measurements are shown in Fig. 1. The low-energy limit, 0.1 eV, was imposed by the power requirements for the measurements.

The infrared absorptivity is of interest in itself since it allows one to determine the free-electron parameters characterizing the free-carrier absorption part of the spectrum. Of interest are the dc conductivity and the electron relaxation time  $\tau$ . To determine these parameters, one must assume that the absorption is due entirely to free carriers, there being no interband or anomalous-skin-effect contributions. Such an assumption is tenuous for the transition metals since the Fermi level cuts the  $d$  bands. If one ignores anomalous-skin-effect contributions, the free-carrier absorption would be constant ( $A = 2/\omega_p\tau$ ) if  $\omega \ll \omega_p$  and  $\omega\tau \gg 1$ .  $\omega_p$  is the plasma frequency. Deviations from a flat absorption curve could be attributed to interband effects if the conditions on  $\omega$  and  $\tau$  are met. The calculated free-carrier absorption is given in Table I, along with  $\omega\tau$  (4.2 K).<sup>65</sup> Clearly, the simple model is not applicable even at 0.15 eV for V and Mo; for Ta,  $\omega\tau$  is not clearly  $\gg 1$ .

In order to perform a Kramers-Kronig (KK) analysis of the reflectivity data, it is customary to assume a Drude-like behavior at low frequency, below the range of experimental data. This has been done in the present case. While there should be little physical meaning associated with the parameters used for the extrapolations, we do note that below about 0.2 eV, the measured absorptivity

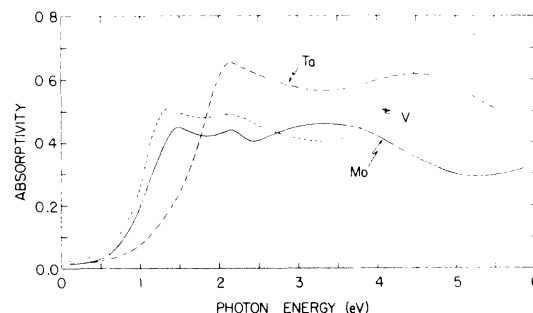


FIG. 1. Low-energy absorptivity of V, Ta, and Mo at  $15^\circ$  angle of incidence. The data to 4.88 eV were taken at 4.2 K.

TABLE I. Free-electron characteristics of the samples. The  $\sigma_0$  and  $\tau$  values were used in the Kramers-Kronig analysis for extrapolation to zero frequency and should not be assigned physical meaning.

Sample	Predicted absorptivity (at 4.2 K)	$\omega\tau^a$ (4.2 K) (at 0.15 eV)	Experimental absorptivity (at 0.15 eV)	$\sigma_0$ ( $10^{14}$ esu)	$\tau$ ( $10^{-14}$ sec)
V	0.00060	22.5	0.0233	500	1.14
Ta	0.00317	4.85	0.0167	800	0.88
Mo	0.00017	76.1	0.0149	1670	1.39

<sup>a</sup>dc resistivities were obtained from Ref. 64.

ties were approximately predicted by the parameters shown in Table I. Again, these parameters were used only for Drude extrapolations to zero frequency.

The absorptivities (Fig. 1) are seen to rise from 0.0233 (V), 0.0167 (Ta), and 0.0149 (Mo) at 0.15 eV. The absorptivity of V displays a first major peak at 1.35 eV. The second peak at 2.15 eV is followed by a broad minimum and a steady rise in  $A$  beyond about 3.3 eV. The first maximum for Ta occurs at 2.15 eV with a wide minimum centered at about 3.4 eV and a second maximum at about 4.6 eV. The absorptivity spectrum of Mo is more complicated: three low energy maxima are evident at 1.5, 2.17, and about 3.3 eV, with minima at 1.85 and 2.45 eV.

The complete reflectivity spectrum of V between 0.1 and 30 eV is shown in Fig. 2. Perhaps the most striking feature is the nearly structureless drop in  $R$  beyond about 3.3 eV. A slight shoulder occurs at about 9–11 eV, which is enhanced at 45° angle of incidence, but none of the striking features observed in Ta and Mo (and Nb<sup>4</sup>) are seen. Above 30 eV, the absorption coefficient has been reported by Sonntag *et al.*,<sup>10</sup> and a calculated reflectivity (assuming the index of refraction  $n$  was unity) displays structure related to core transitions at higher energy.

Our early results on V were compared with those of Seignac and Robin,<sup>9</sup> measured on unannealed films evaporated in a vacuum of  $\sim 10^{-6}$  Torr and transferred in air to their sample chamber. Our reflectivities were consistently lower, no matter how carefully we electropolished. This is inconsistent with all of our previous experience comparing our crystal data with data on films. Finally we gave a sample a very slight polish with 0.3- $\mu$ m diameter Al<sub>2</sub>O<sub>3</sub> just after electropolishing. The resultant data (Fig. 2) are higher than our earlier data, but still below those of Seignac and Robin. (The latter measured at 20° angle of incidence with the polarization of the beam not reported, so comparison is difficult.) Thus we believe that the result of electropolishing V is dissimilar to that for Mo, Ta, and other transition metals we have worked with (Cr, Nb, Zr, Hf, Ti). We are not

confident that the vuv data we present are free of qualitative effects of an oxide overlayer. More will be said about this in a subsequent section. Seignac and Robin<sup>9</sup> observed no strong high-energy structure in V at 20° angle of incidence, but they report a very broad  $R(E)$  shoulder between 15 and 30 eV at 60° angle of incidence. No such feature has been observed in this study at 45° with either  $s$ - or  $p$ -polarized radiation. The difference is difficult to explain.

A comparison of our low-energy absorptivities of V with those calculated from the  $n$  and  $k$  values of Bolotin *et al.*<sup>7</sup> (2 to 9  $\mu$ m) shows good qualitative agreement, though our  $A$  values are considerably lower in magnitude (e. g.,  $A = 0.0233$  vs  $\approx 0.06$  at 0.15 eV). A comparison with the reflectivities of Vilesov *et al.*<sup>8</sup> appears to be fruitless, there being very little agreement at all. The reason for the disagreement is not known; the same apparatus was used subsequently by a different group (Ref. 33), and the results (for Mo) were in good agreement with other studies, including ours.

The reflectivity of Ta is shown in Fig. 3 with the high-energy low-reflectivity region shown enlarged for clarity.  $R(E)$  is almost flat between about 9 and 13 eV, there is a depression centered at about 13.8 eV, and above 16 eV,  $R$  drops quickly. The

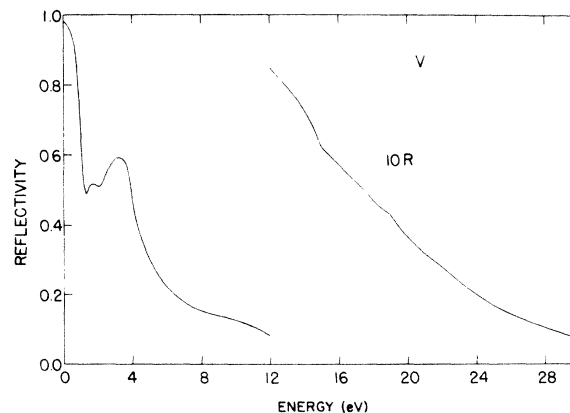


FIG. 2. Reflectivity of vanadium. The scale is expanded to show the high-energy low-reflectivity region more clearly.

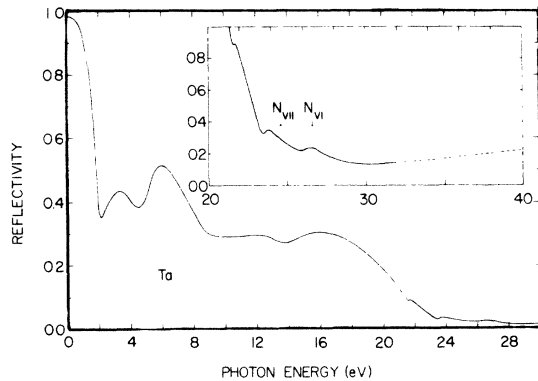


FIG. 3. Reflectivity of Ta. The insert shows the high-energy region and the first few electron volts of the high-energy extrapolation.

insert shows the shoulder at about 21.6 eV as well as two core electron structures at 23.6 and 26.9 eV. The upper limit of our measurements was about 32 eV for Ta, but, as was the case for Nb<sup>4</sup>,  $R$  is rising steadily at 32 eV due to core transitions at higher energies. The dashed line between 32 and 40 eV is part of our high-energy extrapolation based upon the absorption coefficient measurements of Haensel *et al.*<sup>27</sup> The agreement with their results in the region of overlap is good.

A comparison of the present Ta data with the results of Juenker and co-workers<sup>25,26</sup> shows good qualitative agreement. Unfortunately, the group was unable to cover the 5–7-eV range and was limited to discharge lines in the vuv.

The reflectivity of Mo is shown in Fig. 4. Again, the high-energy region is expanded for clarity. For Mo, our upper limit was 37 eV; the dashed line in the insert above 37 eV represents a portion of the high-energy extrapolation. Molybdenum displays a reflectivity spectrum that is very similar to that of Nb and Ta above 8 eV. As was the case for Nb, a shoulder is observed at 7.5 eV (minimum at 7.3 eV, maximum at 7.6 eV) beyond which  $R$  drops sharply to a minimum at 11.2 eV. The minima for Mo (11.2 eV) and Nb (10.3 eV) are deeper than for Ta (approximately 9.5 eV), but the subsequent rise, the shallow valley (centered at about 13, 13.8, and 15.2 eV, respectively) and broad shoulder (16, 16, and 18.8 eV, respectively) are features the three metals share. Further, Mo and Nb have shoulders at about 20.7 and 23 eV which might be related to the more clearly defined rise in Ta at 21.8 eV. Above 30 eV the reflectivity of Mo rises to display two structures at 32.6 and 35.4 eV. At higher energies, further core transitions can be expected, but no optical measurements have yet been performed in that spectral region.

Below about 5 eV, the reflectivity spectrum of

Mo has been studied by a variety of workers. Most agree qualitatively with the spectrum shown in Figs. 1 and 4. Quantitative agreement is also rather good between our work and that of Kirillova *et al.*<sup>33</sup> with only slight allowances made for temperature dependences. The vuv spectra obtained by the different groups are less in agreement. Most, but not all, have observed a deep minimum near 11 eV, but the paths leading to the minimum are diverse. The early work by Kapitsa, Udoyev, and Shirokikh<sup>35</sup> reported what appeared to be erroneously low  $R(E)$  values with less structure at low energy and the minimum at 8 instead of 11 eV. In a more recent study, Udoyev, Koz'yakova, and Kapitsa<sup>36</sup> reported a spectrum which is in good quantitative agreement with ours below about 4 eV and qualitatively agrees above 4 eV (though the dip near 7.5 eV is less pronounced). The early work by Kirillova *et al.*<sup>34</sup> also reported an  $R(E)$  spectrum in quite good agreement with ours, though they observed no structure at 7.5 eV. Kress and Lapeyre,<sup>37</sup> on the other hand, showed only washed-out features below 3.5 eV, the 5.4-eV peak apparently shifted to about 4.5 eV, and  $R$  values as much as 0.3 below ours (6 eV). The common dip near 11 eV was nonetheless observed. It is interesting to note that at 8 eV, the literature boasts such diverse reflectivities as 0.64 (Refs. 25 and 26), 0.53 (Ref. 34 and present work), about 0.43 (Ref. 36), about 0.33 (Ref. 37), and 0.09 (Ref. 35).

The reflectivity spectra presented in Figs. 1–4 have been subjected to KK analyses to determine the optical constants. Since the integral calls for  $R(E)$  over an infinite range of energies, it has been necessary to introduce Drude-like behaviors at low energy and to rely upon other measurements and extrapolations at very high energy. The Drude parameters used in the analysis were shown in Table I and have been discussed earlier. For the high-energy extrapolations, existing absorption mea-

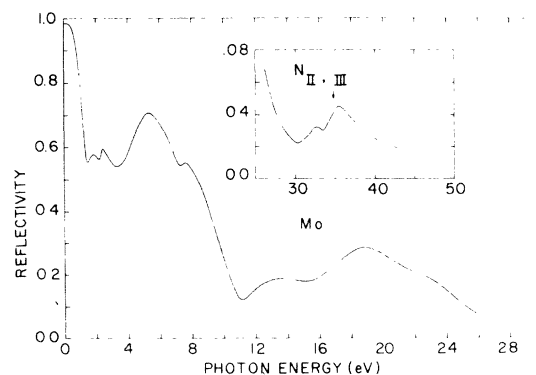


FIG. 4. Reflectivity of Mo. The insert shows the high-energy region. The dashed line represents an extrapolation to high energy.

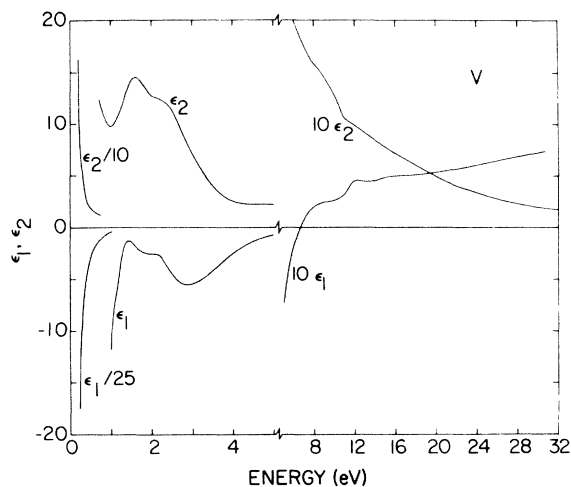


FIG. 5. Dielectric functions of V. The scales are shown expanded for clarity.

measurements for V<sup>10</sup> and Ta<sup>27</sup> were used to 300 and 600 eV, respectively. To extend the range still further, it was assumed that  $R$  could be described by  $R(E) = R_0 E^{-\beta}$ , where the data of the DESY group<sup>10,27</sup> were used to determine  $\beta$  at the highest energies. A value of 2.09 was used for Ta (fitted to calculated  $R$  at 400 and 600 eV, assuming  $n=1$ ) and 4.1 for V (fitted to  $R$  at 190 and 300 eV). The high-energy cutoff was taken to be 1000 eV where  $R$  was  $1.4 \times 10^{-8}$  (V) and  $1.7 \times 10^{-6}$  (Ta). It might be noted that for Ta the reflectivities at 190 and 300 eV could be fitted with a  $\beta$  of 2.84, while 4.1 was needed for V at those same energies. It is apparent that an inverse fourth law does not necessarily describe the high-energy reflectivities of these metals.

While high-energy measurements were available for V and Ta, no such data existed for Mo. It was necessary to introduce extrapolations above about 40 eV. Exponential decays were assumed of a variety of forms, as were various "by-eye" extrapolations. Certainly, no claims can be made as to the uniqueness of the extrapolation upon which our dielectric constants are based. We do note, however, that a  $\beta$  of 3.5, which was the ultimate choice, gave a high-energy  $R(E)$  spectrum which lay between those of V and Ta and, more importantly, produced low-energy  $n$  and  $k$  values which were in good agreement with those of Ref. 33. [The energies near 1 and 2.4 eV were chosen as "fit" points since their calculated  $R(E)$  agreed with ours at those energies; their data thereby represent an independently determined set of dielectric constants.] Because of the uncertainty in the extrapolations, we must assign a greater uncertainty in the magnitudes of the Mo dielectric function than for either V or Ta.

As a partial test of the KK analysis, the resultant dielectric functions were used to compute the reflectivity at 45° (and 60° for Ta) for  $s$  and  $p$  polarizations, with a correction for the imperfect polarization. Agreement with our measured values was within 10% below 20 eV, decreasing to 50% at 30 eV in some cases, although  $R$  is small there.

In Fig. 5 we display the real and imaginary parts of the dielectric function of V. The scales have been expanded to emphasize certain structural aspects. At low energy,  $\epsilon_2$  displays a basically free-electron-like behavior, but above 0.95 eV, interband effects are clearly dominant. Two strong structures in  $\epsilon_2$  have peaks at 1.60 and 2.35 eV. At higher energies, only a weak structure can be observed in  $\epsilon_2$  at about 9 eV. The real part of the dielectric function,  $\epsilon_1$ , is seen to rise steeply at low energy, display maxima at 1.4 and 2.05 eV, with minima at 1.9 and about 2.8 eV before crossing the axis at 6.6 eV. Again, a structure can be seen at about 10 eV.

We could not compare our reflectivity for V with that of Ref. 9 because of angle and polarization differences, but a comparison of  $\epsilon_2$  is possible. That of Ref. 9 is some 40–50% higher above 8 eV, the only range where comparison is possible. The difference could be related to an oxide layer on our sample which would make  $R$  and  $\epsilon_2$  too small. Reference 9 reports a shoulder in  $\epsilon_2$  at about 9 eV which is similar to that shown in Fig. 5. Because of oxide difficulties for V, we feel the data of Ref. 9 are superior to ours above 5 or 6 eV.

The dielectric function of Ta is shown in Fig. 6. The low energy region again is characterized by free-carrier-like  $\epsilon_1$  and  $\epsilon_2$ .  $\epsilon_2$  passes through a minimum at 1.85 eV with interband peaks at about 3.1 and 5.25 eV and a minimum at 4.4 eV. The very broad flat region in  $\epsilon_2$  around 9 eV corresponds to the flat region in the reflectivity in the same energy range. Above about 20 eV, the effects of core transitions can be seen at 21.8, 23.8,

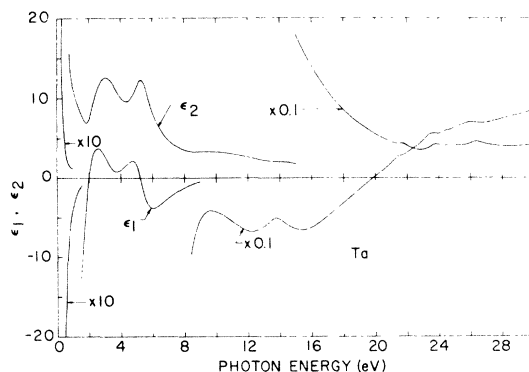


FIG. 6. Dielectric functions of Ta. The scales are shown expanded for clarity.

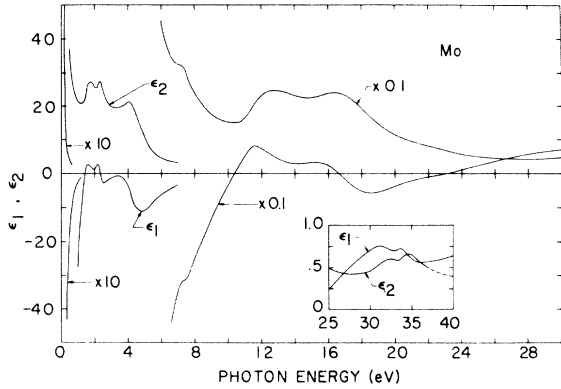


FIG. 7. Dielectric functions of Mo. The high-energy region is shown enlarged in the insert.

and about 26.4 eV.  $\epsilon_1$  displays peaks at 2.65, 4.8, 9.7, 13.8, 21.6, 23.6, and 26 eV with zero crossings at 2.0, 5.22, and finally 19.9 eV.

The dielectric function of Mo is shown in Fig. 7. Considerable resemblance can be seen with the features of Nb<sup>4</sup> above 6 eV. Strong interband absorption is apparent at low energies with the first minimum in  $\epsilon_2$  at 1.25 eV; peaks at 1.8, 2.35, 4.1, about 12.8 and 16.5 eV; a shoulder at about 7.3 eV; and minima appearing 2.1, 3.3, 10.5, and about 15 eV.  $\epsilon_1$  likewise displays complicated structure (peaks at 1.6, 2.2, 3.4, 11.6, 15.5 eV; minima at 1.95, 2.55, 4.9, about 14, and about 18.6 eV; a kink at 7.5 eV; zero crossings at 1.45, 2.35, 10.4, 16.6, and finally 23.2 eV).

Certain sum rules are generally appealed to when considering optical constants. One typically calculates the number of electrons contributing to optical absorption below an energy  $E$  from the oscillator strength sum rule

$$N_{\text{eff}}(E) = \frac{2}{\pi} \frac{1}{(\hbar\omega_p)^2} \int_0^E \epsilon_2(E') E' dE' ,$$

where  $\hbar\omega_p$  is the free-electron plasma energy.  $N_{\text{eff}}$  is shown for Ta, V, and Mo in Fig. 8. The above integral was evaluated from 0.1 eV to  $E$  for use in Fig. 8. The range below 0.1 eV contributes an additional  $(2/\pi) (m_0/m^*) z \tan^{-1} [(0.1 \text{ eV})\tau/\hbar]$ , where we assume  $z$  electrons per atom of effective mass  $m^*$  are in the conduction band, and interband transitions are negligible. At 4 K this is close to  $z(m_0/m^*)$ , even for Ta. Because we do not know  $m^*$ , we have omitted this term in Fig. 8. In Ta we observed the onset of core transitions as low as 24 eV so one would expect  $N_{\text{eff}}$  to rise steadily, beginning at 24 eV. The interband transitions from the valence band, if exhausted at 24 eV, would place this rise on a plateau of 5 electrons per atom, roughly what is seen in Fig. 8. Molybdenum has 6  $e/\text{at.}$  and the core transitions appear at higher energy. For Mo,  $N_{\text{eff}}$  reaches 6  $e/\text{at.}$  at about

30 eV; core effects are noted near 33 eV (Fig. 7). For V, it is clear that very few of the available 5  $e/\text{at.}$  have been involved in optical absorption even at 30 eV where  $N_{\text{eff}}$  has only reached 2.2  $e/\text{at.}$  This is in agreement with the structureless dielectric function shown in Fig. 5.  $N_{\text{eff}}$  for V is shown to be much higher in Ref. 9, reaching 3.6  $e/\text{at.}$  at 30 eV, despite the fact that  $\epsilon_2$  was reported to be only 40–50% higher above 8 eV. The difference in  $N_{\text{eff}}$  between Fig. 8 and Ref. 9 is large even at 1 eV and must be partly due to including the 0–0.1-eV range in the integral reported in Ref. 9.

#### IV. DISCUSSION

Interpretation of features in the dielectric function hinges on the completeness and accuracy of energy-band calculations for the material. Assignments are made according to the energy separation of the bands, the joint density of states (JDOS), and selection rules which allow or forbid the transitions. The observed structure is then related to *regions* of  $\vec{k}$  space separated by the appropriate energy, between which the transitions are allowed and for which the JDOS is large. Photoemission data also give information on the band density of state (DOS). In the optical study in which bands are first related to experimental results, tentative identifications are often based on provisional bands and often without a knowledge of the optical properties of related materials. While the present work is the first detailed discussion of the optical properties of V and Ta (and Mo above  $\sim 5$  eV), we are able to argue from trends observed for the bcc transition metals and on the basis of rather complete (if sometimes differing) energy

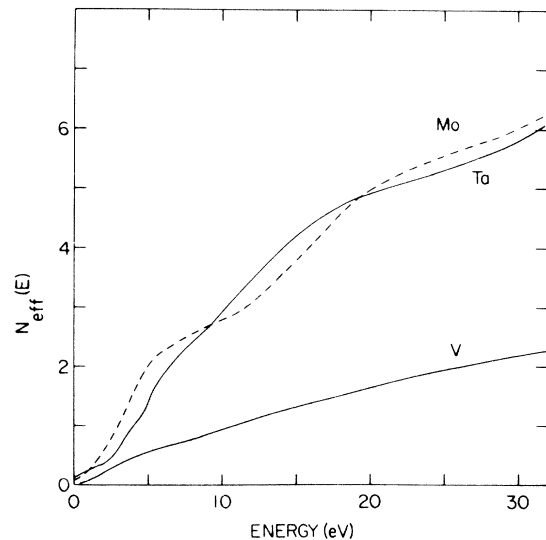


FIG. 8.  $N_{\text{eff}}$  calculated from the oscillator strength sum rule. See text for discussion of low-energy region.

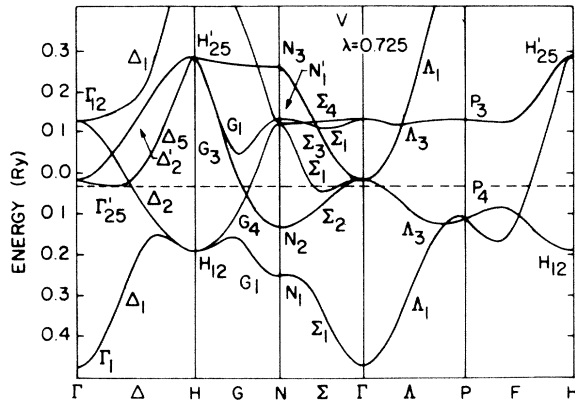


FIG. 9. Energy bands for V calculated by Yasui *et al.* (YHS) (Ref. 17).

bands.

The energy bands of V have been calculated by several groups,<sup>12-18</sup> and, while the bands have basically the same overall shape, important differences exist. These bands often are fit to experiment only at the Fermi level. The investigations of Yasui *et al.*<sup>17</sup> (YHS) and Papaconstantopoulos *et al.*<sup>16</sup> (PAM) showed considerable dependence on the choice of the exchange potential coefficient,  $\alpha$ . For  $\alpha=1$ , YHS showed  $\Gamma'_{25}$  below  $E_F$ ; for  $\alpha=0.725$ , it lay above, in agreement with Refs. 13-16, and 18. Their results also showed  $\Delta_5$  nearly touching the Fermi level while PAM placed it well above  $E_F$ . Finally, YHS display the  $\Sigma_1$  band dipping well below the Fermi energy while PAM show it not touching ( $\alpha=1$ ) and barely touching ( $\alpha=\frac{2}{3}$ ). Self-consistency and the choice of atomic configuration<sup>2,13,16,66</sup> also have been shown to play an important role in the calculations of  $E(\vec{k})$ .

The width of the  $d$  bands is a matter of considerable interest and disagreement. The  $d$ -band width for a bcc lattice is defined as  $E(H'_{25}) - E(H_{12})$ , and a comparison of the different V calculations gives: Mattheiss,<sup>14</sup> 6.5 eV; Hodges *et al.*,<sup>2</sup> 7.9 eV; Snow and Weber,<sup>13</sup> 6.8 eV; YHS, 6.45 eV ( $\alpha=0.725$ ) and 5.4 eV ( $\alpha=1$ ); Anderson *et al.*,<sup>15</sup> (non-self-consistent calculation) 6.8 eV ( $\alpha=1$ ) and 11 eV ( $\alpha=\frac{2}{3}$ ); PAM, 5.5 eV ( $\alpha=1$ ) and 7.27 eV ( $\alpha=\frac{2}{3}$ ); Hattox *et al.*,<sup>18</sup> 6.53 eV.

The agreement of the YHS bands with dHvA data was not discussed, but a comparison with the photoemission results of Eastman<sup>11</sup> showed that their calculated occupied  $d$ -band width,  $E_F - E(H_{12})$ , was only 2.16 eV instead of the measured  $\sim 3$  eV. The agreement of the PAM ( $\alpha=\frac{2}{3}$ ) results was better (3.28 eV), but, as they pointed out, the dHvA agreement was only qualitative (areas 15% smaller than experiment). The agreement would be improved, they reported, by increasing  $\alpha$ . Hattox *et al.*<sup>18</sup> found 3.0 eV for  $E_F - E(H_{12})$ . The differ-

ences in the various V bands are significant and must be borne in mind in the discussion of the electronic properties of V.

The  $E(\vec{k})$  results of YHS for  $\alpha=0.725$  are shown in Fig. 9. The discussion of the electronic properties will be based on Fig. 9 and the  $\alpha=\frac{2}{3}$  bands of PAM.

Unfortunately, the symmetry lines along which the bands are calculated do not sample much of the Brillouin zone. We are forced to discuss inter-band transitions using selection rules and a qualitative JDOS only for limited regions along and, perhaps, near these lines. For metals this can be very misleading, but no JDOS has been calculated for any of these metals. Reference 32 made a limited study of matrix element effects. What is called for is a calculation of  $\epsilon_2$  using matrix elements in all regions of  $\vec{k}$  space. Such calculations for bcc metals are in progress.<sup>67,68</sup>

The behavior of  $\epsilon_2$  for V has been shown to be free-electron-like below about 0.95 eV. Structure then appeared at 1.60 and 2.35 eV. From the bands of Fig. 9, one might expect to find absorption features occurring at very low energy due to  $\Sigma_2 - \Sigma_1$  transitions. As was discussed for Nb,<sup>4</sup> such transitions are forbidden by electric-dipole selection rules. If, however, the spin-orbit effects are strong enough to change the  $\Sigma_1$  and  $\Sigma_2$  bands into  $\Sigma_5$  bands, one might observe weak low-energy effects,  $\Sigma_5 - \Sigma_5$  being allowed. This has not been observed for V, Nb, or Ta.

From the bands of YHS and PAM, it is possible to identify the origin of the first low-energy transition as being due to  $\Sigma_1 - \Sigma_1$  and nearby regions of  $\vec{k}$  space. YHS showed the energy separation to be about 2.0-2.2 eV and PAM agreed with about 2.2 eV (see Table II). Such transitions are allowed and have been identified as the origin of the 2.4-eV structure in  $\epsilon_2$  for Nb.<sup>4</sup> A strong argument supporting the assignment comes from thermomodulation measurements on V and Nb.<sup>23</sup> If the low-energy peak at 1.6 eV for V were due to  $\Sigma_1(E_F) - \Sigma_1$ , then one might expect a strong thermoderivative signal associated with the transition, it being a transition involving the Fermi surface. The thermoderivative signal was very strong and the assignment seems unambiguous. Further support comes from calculations of the band DOS which show a high DOS just below  $E_F$  for Nb<sup>3,66</sup> and Ta,<sup>3,32</sup> and presumably for V also. The lower  $\Sigma_1$  band lies in this high DOS region and the relative shapes of the  $\Sigma$  bands indicates an appreciable JDOS.

While the 1.6-eV peak can be assigned to  $\Sigma_1 - \Sigma_1$  and nearby regions of  $\vec{k}$  space, the identification of the origin of the 2.35-eV peak is less obvious. A comparison of the different V bands shows that the transitions along G may be tentatively associated



TABLE II. Calculated energies over which interband absorption would be expected, occupied and full  $d$ -band width, and experimental results. All energies are given in eV.

	$E(\Sigma_1) - E(\Sigma_1)$	$E(G_1) - E(G_1)$	$E(N_4) - E(N_2)$	$E_F - E(H_{12})$	$E(H'_{25}) - E(H_{12})$
<b>Vanadium</b>					
YHS ( $\alpha = 0.725$ ) <sup>a</sup>	2–2.2	2.7	3.4	2.2	6.45
PAM ( $\alpha = \frac{2}{3}$ ) <sup>b</sup>	2.2	4.0	4.0	3.3	7.27
Eastman <sup>c</sup>				~3	
Snow and Waber <sup>d</sup>				2.9	6.8
Hattox <i>et al.</i> <sup>e</sup>	1.9		3.6	3.0	6.53
This study	1.6	2.35			
<b>Niobium</b>					
Mattheiss (NR) <sup>f</sup>	2.3–2.6	4.5	5.1	3.9	9.0
Oh and Liu (NR) <sup>g</sup>	3.1	4.8	5.7	3.6	9.1
APMS ( $\alpha = \frac{2}{3}$ ) <sup>h</sup>	2.7–3.0	5.0	5.7	4.3	10.3
Brun and Loucks <sup>i</sup>	2.5	4.6	5.4	4.0	9.6
Eastman <sup>c</sup>				~3	
WLO <sup>j</sup>	2.4	4.3	5.1		
<b>Tantalum</b>					
Mattheiss (Rel) <sup>d</sup>	3–3.6	4.6	5.7	3.9	10.2
PV (NR) <sup>k</sup>	2.7–2.9	4.9	5.7	4.1	10.06
This study	3.05	5.25			
<b>Molybdenum</b>					
IH <sup>l</sup>	2.5–2.8	5.2	5.9	6.1	10.4
PV (NR) <sup>k</sup>	2.2	4.9	5.4	5.5	9.25
Eastman <sup>c</sup>				~4.5	
Kress and Lapeyre <sup>m</sup>				~5.5	
This study	2.35	4.1			

<sup>a</sup>See Ref. 17.

<sup>b</sup>See Ref. 16.

<sup>c</sup>See Ref. 11.

<sup>d</sup>See Ref. 13.

<sup>e</sup>See Ref. 18.

<sup>f</sup>See Ref. 3.

<sup>g</sup>See Ref. 67.

<sup>h</sup>See Ref. 66.

<sup>i</sup>T. O. Brun and T. L.

Loucks (unpublished).

<sup>j</sup>See Ref. 4.

<sup>k</sup>See Ref. 32.

<sup>l</sup>See Ref. 55.

<sup>m</sup>See Ref. 37.

with the peak in V as well as low energy features in Nb, Mo, and Ta (Table II). The YHS bands provide few other candidates at less than about 2.5 eV, but PAM's calculations do show bands which might contribute to absorption.  $G_1 \rightarrow G_1$  transitions are favored, however, in light of the results for the other bcc transition metals. The  $G_1 \rightarrow G_1$  transitions are allowed, and a high JDOS should be associated with them since they represent a critical point transition. However, since the wave functions at  $G_1$  are largely  $d$  like, matrix elements might show the contribution from this region of  $\vec{k}$  space to be small. Band results for Ta and Nb show a high band DOS near the crest of the  $G_1$  and  $\Delta_1$  bands. Eastman has shown a high optical DOS about 1.6 eV below  $E_F$  which could be associated with the  $G_1$  crest of the YHS bands. Finally, thermomodulation measurements<sup>23</sup> have shown that the 2.35-eV peak is relatively weak and probably does not involve states near the Fermi level, thereby ruling out some low-energy candidates.

Discussion of the high-energy features of V will be deferred until after the low-energy features of

Ta and Mo have been discussed.

The energy bands of Ta are shown in Fig. 10 and were calculated by Mattheiss.<sup>3</sup> Nonrelativistic Ta bands were also reported by Petroff and Viswanathan<sup>32</sup> (PV) extending to about 20 eV above  $E_F$ . Both employed the APW formalism and their overall agreement is quite good. Both studies calculated the band DOS showing regions of high density just below  $E_F$ , about coincident with the flat  $P(D)N$  band, and about on a level with the  $G_1$  and  $\Delta_1$  crests.

Structure in the dielectric function of Ta appeared at 3.05 and 5.25 eV (Fig. 6). There was an absence of any structure in the absorptivity (Fig. 1) in the very low-energy region, although it was suspected that perhaps spin-orbit splitting would be sufficient to make  $\Sigma_5 \rightarrow \Sigma_5$  transitions possible. That spectral region was carefully examined, but no structure was observed. The origin of the first strong  $\epsilon_2$  structure can be related to the  $\Sigma_1 \rightarrow \Sigma_1$  transitions. Mattheiss showed the energy separation to be about 3–3.6 eV and PV reported 2.7–2.9 eV.



lying bands. The corresponding W and Ta bands show basically the same features, and, on the basis of the rigid-band model, one might expect the same for Nb. Again, the agreement of the PV bands with photoemission results is good. Direct comparison can be made with the band DOS shown in Fig. 13 if matrix element effects are neglected. The PV bands place the 3.6-eV DOS peak<sup>11</sup> between the crest of  $G_1$  and  $\Delta_1$ .

The first peak in  $\epsilon_2$  for V, Nb, and Ta has been related to  $\Sigma_1 \rightarrow \Sigma_1$  transitions, but for Mo the Fermi level (6  $e/at.$ ) lies higher within the  $d$  bands, and one must look elsewhere to account for the 1.8-eV peak. It is generally agreed that the split hybridized bands along  $\Gamma(\Delta)H$  are the source of the structure. IH show the  $\Delta'_2$  and  $\Delta_3$  bands to be 1–2 eV apart. Spin-orbit effects will change this energy difference,<sup>69</sup> but it seems safe to attribute the 1.8-eV peak to transitions in the  $\Delta$  region of  $\vec{k}$  space. From Fig. 7 it can be seen that even when  $\epsilon_2$  passes through the first minimum (1.25 eV), its magnitude is large and considerable interband absorption is taking place, in agreement with the onset of  $\Delta$  transitions at about 1 eV.

Low-energy interband transitions have been observed in W near 0.4 eV<sup>70</sup> and have been attributed to transitions between the spin-orbit split  $\Delta_3$  bands. The Mo spin-orbit splitting parameter has been estimated to be only about one fourth of that of W<sup>55,56</sup> and the corresponding splitting of the Mo bands would be less. In addition to the calorimetric measurements, room-temperature reflectivity measurements were made to 0.06 eV to try to observe low-energy structure.<sup>71</sup> No structure was observed.

To account for the 2.35-eV peak in Mo, we return to the  $\Sigma_1$  bands. The energy separation calculated by PV and IH is in good agreement with the experimental value (Table II). The third structure near 4.1 eV can be related to the  $G_1$  transitions although again the predicted energy is higher than the observed energy.

The discussion so far has been concerned only with low-energy features in the dielectric function. In particular, we have shown that for the four bcc transition metals under consideration, one can identify the  $\Sigma$ ,  $G$ , and possibly  $P(D)N$  regions of  $\vec{k}$  space as probably responsible for structure below  $\sim 6$  eV. Above  $\sim 6$  eV, such identifications become more tenuous.

In their study of Ta, Mo, and W, PV calculated  $E(\vec{k})$  to  $\sim 20$  eV above  $E_F$ . (See Fig. 12.) There is a fairly flat band about 11–12 eV above  $E_F$ , a band composed largely of  $f$ -like states. They showed that for about 7 eV above  $H'_{25}$  the band DOS was low;  $H'_{25}$  was placed about 3.75 eV above  $E_F$ . On the basis solely of the band DOS of Fig. 13, disregarding matrix element effects and selection rules, one

might expect strong absorption between 0 and 9 eV, corresponding to transitions from the conduction bands into the unoccupied  $d$  bands. A region of relatively weak optical absorption about 2 eV wide would follow. Absorption would again be expected for  $\hbar\omega = 11$ –16 eV, corresponding to transitions into the region of high DOS arising from the high-lying flat band, the width of the absorption band being determined by the width of the occupied  $d$  bands and the width of the high-energy peak in the DOS. (The width shown in Fig. 13,  $\sim 5$  eV, may not be as accurate as other features in this figure due to poorer convergence of high-energy bands.) From Fig. 7 it can be seen that indeed between  $\sim 9$  and 11.5 eV, there is only weak absorption, and a strong absorption band is apparent starting at 11.5 eV and extending to  $\sim 18$  eV. Our "optical" occupied  $d$  bandwidth is then  $\sim 6.5$  eV, treating the upper DOS peak as a  $\delta$  function, and  $\sim 4.1$  eV treating the observed bandwidth  $\Delta E$  as  $\Delta E = [(\Delta E_d)^2 + (\Delta E_u)^2]^{1/2}$  with  $\Delta E_d$  the width of the filled  $d$  band and  $\Delta E_u$  the width of the DOS peak above  $E_F$ . The PV bands give a value of  $\sim 5.5$  eV and photoemission studies give  $\sim 4.5$  eV<sup>32</sup> and 5.5 eV.<sup>37</sup> While it is not possible to identify the broad features in  $\epsilon_2$  with any particular region of  $\vec{k}$  space, it appears reasonable to attribute the high-energy absorption to transitions with final states in the high-lying bands with a high density of states. The observed shape will require matrix elements for its explanation.

A similar simple argument can be made for Ta, again based on the calculations of PV. The  $d$  bands extend  $\sim 3.5$ –4 eV below  $E_F$  and the region of low DOS appears between about 6 and 12 eV above  $E_F$ , with a greater magnitude than in Mo. Structure would be expected in the first 10 eV with a minimum about 2 eV wide and a region due to high-energy transitions about 4 eV wide. This is only very roughly realized in the experimental features

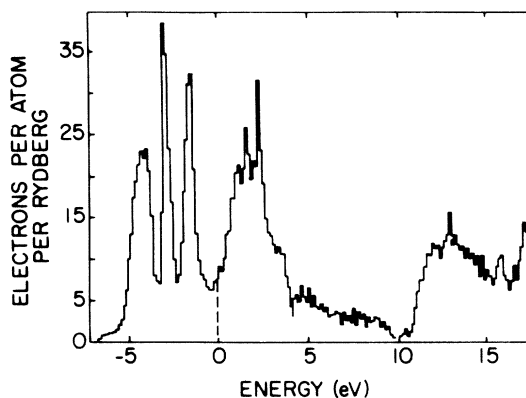


FIG. 13. Band density of states for Mo calculated by Petroff and Viswanathan (PV).

TABLE III. Loss functions and plasmon parameters in bcc transition metals. All energies in eV. Empty spaces mean no data available.

	Metal Electrons/atom	V 5	Nb 5	Mo 6	Ta 5
Calculated	free-electron $\hbar\omega_p^a$	22.32	19.62	23.08	19.65
	$\hbar\omega_p/\sqrt{2}$	15.78	13.87	16.32	13.89
From electron- energy-loss measurements	electron energy loss near $\hbar\omega_p$	24.0 <sup>b</sup> 16.5 <sup>b</sup>	19.7 <sup>c</sup>	22.4 <sup>c</sup>	20.4 <sup>c</sup>
	“lowered” electron energy loss	10.5 <sup>b</sup> 5.1 <sup>b</sup>	9.9 <sup>c</sup>	10.1 <sup>c</sup>	10.1 <sup>c</sup>
From previous optical data	peak in $\text{Im}(-1/\tilde{\epsilon})$	20.6 <sup>d</sup>			
	lower peak in $\text{Im}(-1/\tilde{\epsilon})$	7.5 <sup>e</sup>			
	peak in $\text{Im}[-1/(\tilde{\epsilon})]$				
	lower peak in $\text{Im}[-1/(\tilde{\epsilon}+1)]$	7.0 <sup>e</sup>	7.1 <sup>e</sup>	9.9 <sup>f</sup>	
Present work	peak in $\text{Im}(-1/\tilde{\epsilon})$	18.4	20.8 <sup>g</sup>	24.4	20.7
	lower peak in $\text{Im}(-1/\tilde{\epsilon})$	11.0	9.7 <sup>g</sup>	10.4	~8.9
	peak in $\text{Im}(-1/(\tilde{\epsilon}+1))$	10.0	17.7 <sup>g</sup>	19.8	17.2
	lower peak in $\text{Im}[-1/(\tilde{\epsilon}+1)]$	5.2	9.0 <sup>g</sup>	9.5	~8.6

<sup>a</sup>Atomic volumes from K. Gschneider, Solid State Phys. **16**, 275 (1964).  
<sup>b</sup>Reference 79.

<sup>c</sup>Reference 74.  
<sup>d</sup>Reference 9.  
<sup>e</sup>Reference 8.

<sup>f</sup>Reference 37.  
<sup>g</sup>Reference 4.

of Fig. 6. Strong absorption is apparent in the first 7 eV and slight features appear near 10 and 14.5 eV, but the region of low absorption is less clearcut than in Mo. It is possible that strong relativistic effects in Ta (ignored by PV) would strongly alter the high-energy bands. Matrix elements effects may also play an increasingly important role, though this is difficult to substantiate at this point.

The simple band DOS argument again finds remarkably good success with Nb. The wide absorption features in Nb have maxima at 14.5 and 13.8 eV.<sup>4</sup> If a rigid-band model is applied to the band DOS of Mo,  $E_F$  is shifted to lower energy by about 1.5 eV. One would then expect strong absorption below about 7.5 eV, a 2-eV wide dearth of absorption, then a 5–6.5-eV wide high-energy absorption band. This is in good agreement with the observed dielectric function.

Nb and Mo share a common feature in  $\epsilon_2$  at about 7.5 eV. It is difficult to identify unambiguously the origin of the structure. Possible regions which could contribute are the nearly parallel bands along  $\Delta_1 \rightarrow \Delta_1$  and  $\Lambda_1 \rightarrow \Lambda_1$  and the region near  $N$ .

At very high photon energies, it is possible to excite core electrons, the resulting features being easily related to atomic energy levels.<sup>72</sup> The core levels of V lie beyond the range of our measurements,<sup>10,72</sup> but high-energy features in Ta and Mo have been observed. In Ta, structure in  $\epsilon_2$  appeared at 23.6 and 26 eV, corresponding to excitations of the  $N_{VII}$  and  $N_{VI}$  electrons. Core effects have been observed in Mo at 32.4 and 34.6 eV, corresponding to the  $N_{II,III}$  levels.

The spectrum of energy loss by fast electrons traversing a solid sample is proportional to the loss functions  $\text{Im}(-1/\tilde{\epsilon})$  for losses due to creating volume excitations, and  $\text{Im}[-1/(\tilde{\epsilon}+1)]$  for losses due to creating surface excitations. The use of our dielectric functions in these loss functions gives the loss spectra for long wavelength excitations, both single particle and collective, in the solid. Peaks in  $\text{Im}(-1/\tilde{\epsilon})$ , where  $\epsilon_2$  is small,  $d\epsilon_2/dE < 0$  and  $d\epsilon_1/dE < 0$  usually signify the excitation of bulk plasmons. Roughly similar criteria hold for surface-plasmon peaks in  $\text{Im}[-1/(\tilde{\epsilon}+1)]$ . For a free-electron gas, volume plasmons occur at  $\hbar\omega_p$ , and surface plasmons at  $\hbar\omega_p/\sqrt{2}$ .

Characteristic energy-loss measurements<sup>73–79</sup> on bcc transition metals often have been interpreted in terms of a free-electron gas model, for loss peaks do appear at energies near a plasma energy calculated by treating the  $s$  and  $d$  electrons as free. Since the measurements of the loss spectrum usually have involved fast electrons reflected from thick samples instead of studies of the angle and thickness dependence of losses suffered by electrons transmitted through thin, unsupported films, it has not been possible to identify properly<sup>80</sup> structure in the loss spectra. The volume and surface electron-energy-loss functions have not been obtained and the correlation of observed spectrum with the free-electron gas predictions has been ambiguous.

The loss functions for V, Ta, and Mo are shown in Figs. 14–16. Table III gives the peaks in these functions, along with those for Nb,<sup>4</sup> free-electron-gas plasmon energies, and electron-energy-loss

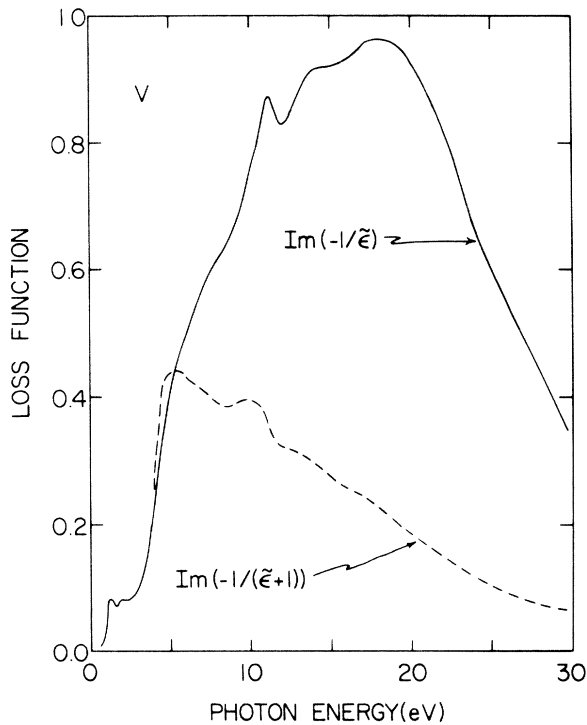


FIG. 14. Volume  $\text{Im}(-1/\bar{\epsilon})$  and surface  $\text{Im}[-1/(\bar{\epsilon}+1)]$  loss functions of V, shown solid and dashed, respectively.

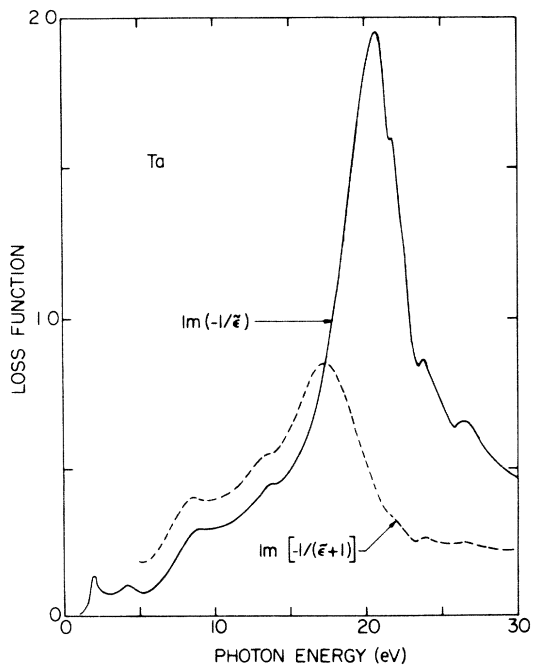


FIG. 15. Volume (solid) and surface (dashed) loss functions of Ta. The surface loss scale has been shifted by +0.1 for clarity.

peak positions. Structure at low energy, below about 5 eV, can be related to structure in the dielectric functions themselves.

From Figs. 14–16 and Table III the following can be seen:

(i) All these metals have a volume-plasmon energy close to the free-electron value. This energy is well above the region of strong interband absorption, so the proximity to the free-electron value is not a complete surprise. These peaks in  $\text{Im}(-1/\bar{\epsilon})$  can be safely identified as due to volume plasmons for, at the energy of the peaks,  $\epsilon_1$  and  $\epsilon_2$  are both small,  $d\epsilon_1/dE > 0$ , and  $d\epsilon_2/dE < 0$ .

(ii) The low-energy peaks in  $\text{Im}(-1/\bar{\epsilon})$  also have the characteristics of volume-plasmon resonances, albeit the damping is large and the background is high relative to the peak heights. These metals then seem to exhibit two types of volume plasmons, a phenomenon not previously known. The imaginary part of the dielectric function shows a minimum around the lower-energy plasmon, the minimum value being between 1.0 and 2.5.

(iii) There are often two peaks in  $\text{Im}[-1/(\bar{\epsilon}+1)]$ , each of which seems to arise from a surface plasmon, both of which are strongly damped. This damping makes calling the excitation at this energy a plasmon questionable in some cases (e.g., the lower-energy peak in Ta). In no case are any of these peaks near  $\hbar\omega_p/\sqrt{2}$ . The low-energy peak, like that in  $\text{Im}(-1/\bar{\epsilon})$ , occurs in the region of a relative minimum of  $\epsilon_2$ .

(iv) In many cases the loss peak previously iden-

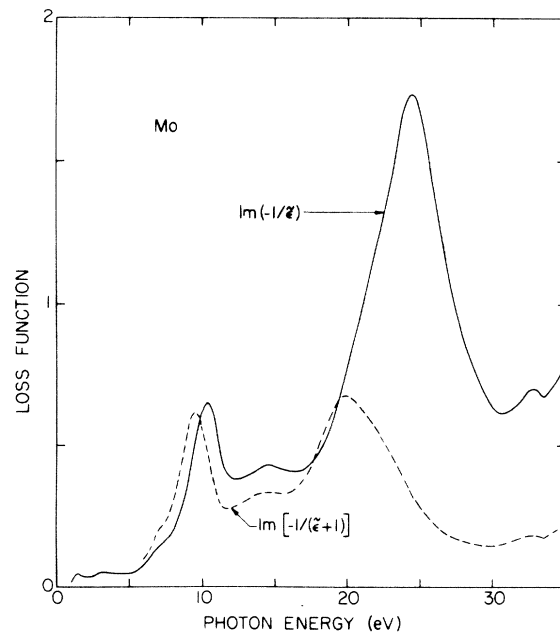


FIG. 16. Volume (solid) and surface (dashed) loss functions of Mo.

tified as a surface plasmon because of its lower energy is probably a combination of a volume and a surface plasmon, both of which occur at nearly the same energy.

The foregoing statements are difficult to justify for V from our data alone. The major effect of an oxide film is a change in the heights of peaks in  $\text{Im}(-1/\bar{\epsilon})$  and a change in positions, shapes, and heights of peaks in  $\text{Im}[-1/(\bar{\epsilon}+1)]$ . Our volume loss function for V resembles that of Ref. 9, but it is not similar enough to our loss functions for Nb, Mo, and Ta, in our view. Small errors in  $\bar{\epsilon}$  can distort the loss function. The best loss functions for V are, we feel, those of Ref. 79, although we disagree with the interpretation given there. Comparison of Ref. 79 with our Fig. 14 leads us to conclude the volume plasmons occur at 24.0 and 10.5 eV in V, with surface plasmons at 16.5 and 5.1 eV (peak positions from Ref. 79). Thus in Ref. 79, the two loss peaks that disappear upon oxidation of a clean surface are due to surface plasmons.

Our results for Mo indicate two volume plasmons, at 24.4 and 10.4 eV, and two surface plasmons, at 14.8 and 9.5 eV. For Ta the two volume plasmons are at 20.7 and  $\sim 8.9$  eV and the surface plasmons at 17.2 and  $\sim 8.6$  eV. Apholte and Ulmer<sup>74</sup> reported characteristic energy-loss peaks (at 2000 K) at  $22.4 \pm 0.7$  and  $20.4 \pm 1.2$  eV for Mo and Ta, respectively. The results of Lynch and Swan<sup>75</sup> also showed peaks at 22.8 eV (Mo) and 19.6 eV (Ta). They also reported structures at lower energies, but not at the energies predicted by the free-electron-gas  $1/\sqrt{2}$  relation of bulk to surface plasmon energy. Nonetheless, they attributed a clearly defined peak near 10 eV (Mo) and a less well-defined peak at about the same energy (Ta) to surface losses. Reference 74 also observed structure at  $10.1 \pm 1.2$  eV (Ta) and  $10.1 \pm 0.5$  eV (Mo), but they were unable to separate volume from surface losses.

The volume plasmon at higher energy is close to the free-electron-gas value, but the higher-energy surface loss peak is not. The observed volume plasmon then probably corresponds to the collective motion of all the valence (*s* and *d*) electrons in the solid. The associated surface plasmon is shifted from  $\hbar\omega_p/\sqrt{2}$  by interband transitions which occur near  $\hbar\omega_p/\sqrt{2}$  with considerably more strength than at  $\hbar\omega_p$ . This can be viewed as a screening of the Coulomb force by the valence electrons (or antiscreening if the frequency is increased). The volume plasmon at lower energy probably involves only a group of electrons; perhaps the core charge density of the *d*-like electrons does not participate. Clearly we do not have a free-electron situation in these metals, although one type of collective mode behaves nearly as the corresponding mode in a

free-electron gas.

A recent theory<sup>81</sup> for the long-range part of the surface energy of metals associates this energy with the shift in energy of plasmon modes when a pair of surfaces is created. The only material parameter in this theory for free-electron-like metals is the plasma energy  $\hbar\omega_p$ , the surface plasmon energy being  $\hbar\omega_p/\sqrt{2}$ . The theory also was applied to transition metals with impressive success, the plasma frequencies usually being obtained from the most stable oxidation state of the metals.

The volume plasmon energies used by Schmit and Lucas were nearly in agreement with experiment, but their surface-plasmon energies were not. The long-range (plasmon) contribution to the surface energy is given by

$$\sigma = \frac{\sqrt{2}-1}{16\pi} \hbar\omega_p k_c^2, \quad ,$$

where  $k_c$  is the surface-plasmon cutoff wave vector. The factor  $(\sqrt{2}-1)\hbar\omega_p$  corresponds to the shift of equal numbers ( $\propto k_c^2$ ) of collective modes from energies 0 and  $\hbar\omega_p$  to  $\hbar\omega_p/\sqrt{2}$  as the surfaces are created. If we call  $E$  the volume plasmon energy and  $\alpha E$  the lower surface-plasmon energy, the above factor is replaced by  $(2\alpha-1)E$ . With the energy of the high-energy volume loss peak as  $E$  and that of the low-energy surface loss peak as  $\alpha E$ , the above factor is very small, even going negative for some metals. Use of the high-energy surface loss peak makes  $\sigma$  too large, as does using all four peaks, unless  $k_c$  is adjusted downward. Thus when the actual collective mode frequencies are used, the Schmit-Lucas model is in very poor agreement with experimental surface energies for the bcc transition metals. It is likely that the "Begrenzung" sum rule used in Ref. 81 is at fault. The number of volume collective modes lost does not equal the number of surface *collective* modes gained, but only the number of surface modes of all types. The surface modes in bcc transition metals are clearly strongly damped. It is likely that the loss of volume collective modes is compensated for by an increase in some surface single-particle modes and modes of mixed character as well as surface collective modes, but these new modes need not all have the same energy. Surface-mode damping occurs in a free-electron gas,<sup>82</sup> for the surface plasmons always have components of wave vector normal to the surface that exceed  $k_c$ , coupling the surface collective modes to single-particle modes. The value of  $k_c$  to use in the Schmit-Lucas model need not be the same for volume and surface modes. It seems that the formula of Schmit and Lucas gives nearly the correct surface energy in these metals fortuitously. Alternatively, by using a different number of modes of

each type, perhaps one could recover the experimental surface energy when using experimental collective mode energies, abandoning a sum rule for collective modes only.

#### V. CONCLUSION

The reflectivity and dielectric function spectra of V, Ta, and Mo have been discussed in terms of free-electron-like absorption, interband absorption, absorption to a probable high-lying flat band, and core excitation in the respective regions of the spectrum. The occurrence of two surface and two volume plasmons in these metals has been shown and discussed. Finally, comparisons of various band calculations have been made.

#### ACKNOWLEDGMENTS

The authors gratefully acknowledge F. A. Schmidt for providing the starting ingots and annealing the samples; H. H. Baker for lending his

expertise in electropolishing the samples; G. V. Austin, E. L. DeKalb, and N. M. Neymer for performing the chemical analysis; and J. Ostenson for measuring the resistivity ratios. Dr. M. A. Lind generously performed the infrared reflectivity measurements on Mo beyond 10  $\mu\text{m}$ . Discussions with Professor L. Hodges and Professor S. H. Liu were very beneficial. We gratefully acknowledge correspondence with Professor D. W. Juenker and Mme. S. Robin. The cooperation of the storage-ring staff, especially E. M. Rowe, C. H. Pruett, and R. Otte is appreciated. The storage ring is supported by the U. S. Air Force Office of Scientific Research. During the final analysis stages of this work, one of us (J. H. W.) was a Postdoctoral Fellow associated with the Graduate Center for Materials Research, University of Missouri-Rolla. He gratefully acknowledges the computational assistance of C. A. Ward and G. S. Kovener, and the generosity of Professor R. J. Bell and Professor R. W. Alexander.

\*Present address: Physical Sciences Laboratory, University of Wisconsin, Stoughton, Wisc. 53589.

- <sup>1</sup>A great many valuable contributions have appeared in the literature. We will not attempt to summarize those articles, but refer the reader to the review articles by T. L. Loucks, *Augmented Plane Wave Method* (Benjamin, New York, 1967); W. A. Harrison, *Pseudopotentials in the Theory of Metals* (Benjamin, New York, 1966); V. Heine, M. L. Cohen, and D. Weire, in *Solid State Physics*, edited by F. Seitz and D. Turnbull (Academic Press, New York, 1970), Vol. 24.
- <sup>2</sup>L. Hodges, R. E. Watson, and H. Ehrenreich, *Phys. Rev. B* **5**, 3953 (1972).
- <sup>3</sup>L. F. Mattheiss, *Phys. Rev. B* **1**, 373 (1970).
- <sup>4</sup>J. H. Weaver, D. W. Lynch, and C. G. Olson, *Phys. Rev. B* **7**, 4311 (1973).
- <sup>5</sup>J. H. Weaver and D. W. Lynch, *Phys. Rev. B* **7**, 4737 (1973).
- <sup>6</sup>C. G. Olson and D. W. Lynch, unpublished Cr results.
- <sup>7</sup>G. A. Bolotin, A. N. Voloshinskii, M. M. Kirillova, M. M. Noskov, A. V. Sokolov, and B. A. Charikov, *Fiz. Met. Metalloved.* **13**, 823 (1962) [*Phys. Met. and Metallogr.* **13**, No. 6, 24 (1962)].
- <sup>8</sup>F. I. Vilesov, A. A. Azgrubskii, and M. M. Kirillova, *Opt Spektrosk.* **23**, 153 (1967) [*Opt Spectrosc.* **23**, 7a (1967)]. See also M. Kirillova, L. V. Momerovannaya, G. A. Bolotin, V. M. Mayevskiy, M. M. Noskov, and M. S. Bolotina, *Fiz. Met. Metalloved.* **25**, 459 (1968) [*Phys. Met. Metallogr.* **25**, 81 (1968)].
- <sup>9</sup>A. Seignac and S. Robin, *C. R. Acad. Sci. Ser B* **271**, 919 (1970).
- <sup>10</sup>B. Sonntag, R. Haensel, and C. Kunz, *Solid State Commun.* **7**, 597 (1969).
- <sup>11</sup>D. Eastman, *Solid State Commun.* **7**, 1697 (1969).
- <sup>12</sup>L. F. Mattheiss, *Phys. Rev.* **134**, A970 (1964).
- <sup>13</sup>E. C. Snow and J. T. Waber, *Acta Metall.* **17**, 623 (1969).
- <sup>14</sup>L. F. Mattheiss, *Phys. Rev.* **139**, A1893 (1965).
- <sup>15</sup>J. R. Anderson, J. W. McCaffrey, and D. A. Papa-

- constantopoulos, *Solid State Commun.* **7**, 1439 (1969).
- <sup>16</sup>D. A. Papaconstantopoulos, J. R. Anderson, and J. W. McCaffrey, *Phys. Rev. B* **5**, 1214 (1972).
- <sup>17</sup>M. Yasui, E. Hagashi, and M. Shimizu, *J. Phys. Soc. Jap.* **29**, 1446 (1970).
- <sup>18</sup>T. M. Hattox, J. B. Conklin, Jr., J. C. Slater, and S. B. Trickey, *J. Phys. Chem. Solids* **34**, 1627 (1973).
- <sup>19</sup>L. Hodges (private communication).
- <sup>20</sup>N. E. Alekseevskii and V. S. Egorov, *Zh. Eksp. Teor. Fiz. Pis'ma Red.* **1**, 141 (1965) [*Sov. Phys. JETP Lett.* **1**, 141 (1965)].
- <sup>21</sup>K. S. Nelson, J. L. Stanford, and F. A. Schmidt, *Phys. Lett. A* **28**, 402 (1968).
- <sup>22</sup>R. A. Phillips, *Phys. Lett. A* **36**, 361 (1971).
- <sup>23</sup>J. H. Weaver, C. Culp, and D. W. Lynch, (unpublished).
- <sup>24</sup>R. W. Christy (private communication); P. B. Johnson and R. W. Christy, *Phys. Rev. B* **9**, 5056 (1974).
- <sup>25</sup>D. W. Juenker, L. J. LeBlanc, and C. R. Martin, *J. Opt. Soc. Am.* **58**, 164 (1968).
- <sup>26</sup>L. J. LeBlanc, J. S. Farrell, and D. W. Juenker, *J. Opt. Soc. Am.* **54**, 456 (1964).
- <sup>27</sup>R. Haensel, K. Radler, B. Sonntag, and C. Kunz, *Solid State Commun.* **7**, 1495 (1969).
- <sup>28</sup>M. M. Halloran, J. H. Condon, J. E. Graebner, J. E. Kunzler, and F. S. L. Hsu, *Phys. Rev. B* **1**, 336 (1970).
- <sup>29</sup>A. C. Thorson and T. G. Berlincourt, *Phys. Rev. Lett.* **7**, 244 (1971).
- <sup>30</sup>G. B. Scott, M. Springford, and J. R. Stockton, *Phys. Lett. A* **27**, 655 (1961).
- <sup>31</sup>E. Fawcett, W. A. Reed, and R. R. Soder, *Phys. Rev.* **159**, 533 (1967).
- <sup>32</sup>T. Petroff and C. R. Viswanathan, *Phys. Rev. B* **4**, 799 (1971).
- <sup>33</sup>M. M. Kirillova, L. V. Nomerovannaya, and M. M. Noskov, *Zh. Eksp. Teor. Fiz.* **60**, 2252 (1971) [*Sov. Phys. JETP* **33**, 1210 (1971)]. See also M. M. Kirillova, G. A. Bolotin, and V. M. Mayevskii, *Fiz. Met.*

- Metalloved 24, 95 (1967) [Phys. Met. Metallogr. 24, No. 1, 91 (1967)].
- <sup>34</sup>M. M. Kirillova, G. A. Bolotin, and V. M. Mayeykskii, Fiz. Metal. Metalloved. 19, 495 (1965) [Phys. Met. and Metallogr. 19, No. 4, 13 (1965)].
- <sup>35</sup>M. L. Kapitsa, Yu. P. Udoyev, and E. I. Shirokikh, Fiz. Tverd. Tela 11, 816 (1969) [Sov. Phys.-Solid State 11, 665 (1969)].
- <sup>36</sup>Yu. P. Udoyev, N. S. Koz'yakova, and M. L. Kapitsa, Fiz. Metal. Metalloved. 31, 439 (1971) [Phys. Met. Metallogr. 31, No. 2 229 (1971)].
- <sup>37</sup>K. A. Kress and G. J. Lapeyre, J. Opt. Soc. Am. 60, 1681 (1970). See also K. A. Kress and G. J. Lapeyre, Natl. Bur. Stand. Spec. Publ. No. 323 (U. S. GPO, Washington, D. C., 1970).
- <sup>38</sup>J. Anderson, G. W. Rubloff, and P. J. Stiles, Solid State Commun. 12, 825 (1973).
- <sup>39</sup>B. W. Veal and A. P. Paulikas, Phys. Rev. B (to be published).
- <sup>40</sup>D. D. Koelling, F. M. Mueller, and B. W. Veal, Phys. Rev. B (to be published).
- <sup>41</sup>J. A. Hoekstra and J. L. Stanford, Phys. Rev. B 8, 1416 (1973).
- <sup>42</sup>D. M. Sparlin and J. A. Marcus, Phys. Rev. 144, 484 (1965).
- <sup>43</sup>G. Leaver and A. Meyers, Philos. Mag. 19, 465 (1969).
- <sup>44</sup>V. R. Boiko, V. A. Gasparov, and I. G. Gverdtiteli, Zh. Eksp. Teor. Fiz. 56, 489 (1969) [Sov. Phys. JETP 29, 267 (1969)].
- <sup>45</sup>J. R. Cleveland and J. L. Stanford, Phys. Rev. B 4, 311 (1971).
- <sup>46</sup>E. Fawcett, Phys. Rev. 128, 154 (1962).
- <sup>47</sup>E. Fawcett and W. A. Reed, Phys. Rev. 134, A723 (1964).
- <sup>48</sup>N. E. Alekseevskii, V. S. Egorov, G. E. Karstens, and R. N. Kazak, Zh. Eksp. Teor. Fiz. 43, 731 (1962) [Sov. Phys. JETP 16, 519 (1963)].
- <sup>49</sup>E. Fawcett and D. Griffiths, J. Phys. Chem. Solids 23, 1631 (1962).
- <sup>50</sup>P. A. Bezuglyi, S. E. Zhevago, and V. T. Denisenko, Zh. Eksp. Teor. Fiz. 49, 1457 (1965) [Sov. Phys. JETP 22, 1002 (1966)].
- <sup>51</sup>R. Herrman, Phys. Status Solidi 25, 661 (1968).
- <sup>52</sup>W. M. Lomer, Proc. Phys. Soc. Lond. 80, 489 (1962).
- <sup>53</sup>J. H. Wood, Phys. Rev. 126, 517 (1962).
- <sup>54</sup>W. M. Lomer, Proc. Phys. Soc. Lond. 84, 327 (1964).
- <sup>55</sup>T. L. Loucks, Phys. Rev. 139, A1181 (1965).
- <sup>56</sup>L. F. Mattheiss, Phys. Rev. 139, A1893 (1965).
- <sup>57</sup>R. J. Iverson and L. Hodges, Phys. Rev. B 8, 1429 (1973).
- <sup>58</sup>C. G. Olson and D. W. Lynch, Phys. Rev. B 9, 3159 (1974).
- <sup>59</sup>L. W. Bos and D. W. Lynch, Phys. Rev. B 2, 4784 (1970).
- <sup>60</sup>Characteristic crystallite dimensions were 5 mm (V), 5 mm (Mo-bicrystal), and 2 mm (Ta).
- <sup>61</sup>Analysis showed that C, O, and N were present in the following amounts (ppm), respectively; V (28, 50, 1); Ta (43, 70, 10); Mo (22, 8, 1).
- <sup>62</sup>The samples of V and Mo were electropolished in cooled (by dry ice and acetone) solutions of perchloric acid (6% by volume in methanol). A cooled 2% solution of H<sub>2</sub>SO<sub>4</sub> was used for Ta.
- <sup>63</sup>The samples were annealed for 18 h at 1150 °C (V) and 1650 °C (Mo and Ta).
- <sup>64</sup>For a discussion of surface damage see Ref. 4 and references therein.
- <sup>65</sup>The dc resistivity at room temperature was obtained from G. T. Meaden, *Electrical Resistance of Metals* (Plenum, New York, 1965), and our measurements of the resistivity ratio.
- <sup>66</sup>J. R. Anderson, D. A. Papaconstantopoulos, J. W. McCaffrey, and J. E. Schirber, Phys. Rev. B 7, 5115 (1973).
- <sup>67</sup>K. H. Oh and S. H. Liu (private communication).
- <sup>68</sup>V. Moruzzi (private communication).
- <sup>69</sup>The spin-orbit splitting of the sixfold  $\Gamma_{25}^-$  degeneracy into a doubly degenerate  $\Gamma_7^+$  and a fourfold degenerate  $\Gamma_8^+$  is known to occur. The energy of the  $\Gamma_8^+$  state is roughly 0.1 eV below that of the  $\Gamma_{25}^-$  state for Mo. The spin-orbit splitting of the  $\Delta_5$  bands is expected to be less than at  $\Gamma$ .
- <sup>70</sup>L. V. Nomerovannaya, M. M. Kirillova, and M. M. Noskov, Zh. Eksp. Teor. Fiz. 60, 748 (1971) [Sov. Phys.-JETP 33, 405 (1971)].
- <sup>71</sup>The measurements were kindly performed by Dr. M. A. Lind using a technique described in M. A. Lind, Ph. D. dissertation, (Iowa State University, 1972) (unpublished).
- <sup>72</sup>J. A. Bearden and A. F. Burr, Rev. Mod. Phys. 39, 125 (1967).
- <sup>73</sup>J. L. Robins and J. B. Swan, Proc. Phys. Soc. Lond. 76, 857 (1960).
- <sup>74</sup>H. R. Apherite and K. Ulmer, Phys. Lett. 22, 522 (1966).
- <sup>75</sup>M. J. Lynch and J. B. Swan, Aust. J. Phys. 21, 811 (1968).
- <sup>76</sup>E. A. Bakulin, L. A. Balabanova, M. M. Bredov, E. G. Ostroumova, E. V. Stepin, and V. V. Shcherbinina, Fiz. Tverd. Tela 11, 685 (1969) [Sov. Phys.-Solid State 11, 549 (1969)].
- <sup>77</sup>V. V. Zashkvara, M. I. Korsunskii, V. S. Red'kin, and V. E. Masyagin, Fiz. Tverd. Tela 11, 366 (1969) [Sov. Phys.-Solid State 11, 3083 (1970)].
- <sup>78</sup>L. Fiermans and J. Vennik, Phys. Status Solidi 41, 621 (1970).
- <sup>79</sup>G. W. Simmons and E. J. Scheibner, J. Appl. Phys. 43, 693 (1972).
- <sup>80</sup>H. Raether, Springer Tracts Mod. Phys. 38, 85 (1965).
- <sup>81</sup>J. Schmit and A. A. Lucas, Solid State Commun. 11, 415 (1972); 11, 419 (1972).
- <sup>82</sup>P. J. Feibelman, Phys. Rev. 176, 551 (1968).